JACS
JOURNAL OF THE AMERICAN CHEMICAL SOCIETY
Perspective
pubs.acs.org/JACS

Polymerization-Induced Self-Assembly of Block Copolymer Nano-objects via RAFT Aqueous Dispersion Polymerization

Nicholas J. Warren and Steven P. Armes*

Department of Chemistry, University of Sheffield, Brook Hill, Sheffield, Yorkshire S3 7HF, U.K.

ABSTRACT: In this Perspective, we discuss the recent development of polymerization-induced self-assembly mediated by reversible addition−fragmentation chain transfer (RAFT) aqueous dispersion polymerization. This approach has quickly become a powerful and versatile technique for the synthesis of a wide range of bespoke organic diblock copolymer nano-objects of controllable size, morphology, and surface functionality. Given its potential scalability, such environmentally-friendly formulations are expected to offer many potential applications, such as novel Pickering emulsifiers, efficient microencapsulation vehicles, and sterilizable thermo-responsive hydrogels for the cost-effective long-term storage of mammalian cells.

INTRODUCTION

The seminal discovery of living polymerizations by Szwarc and co-workers in 1956 provided the synthetic means to prepare well-defined block copolymers.[1,2] Within just a few years, the first reports on block copolymer self-assembly were published,[3,4] which ultimately led to the emergence of an industrially-relevant interdisciplinary topic that spans polymer chemistry, polymer physics, and polymer engineering. For example, self-assembly of ABA triblock copolymers in the solid state is the basis for thermoplastic elastomers (synthetic rubber),[5,6] while block copolymers based on alkylene oxides are widely used in various commercial formulations as surfactants, dispersants, gelators, and stabilizers.[7] More recently, block copolymer self-assembly in solution has been extensively studied by groups led by Eisenberg, Bates, Discher, and Kataoka.[8−12] Potential applications in the field of drug and gene delivery have been a particular recent focus.[11,13−15]

In principle, amphiphilic diblock copolymers can form a wide range of particle morphologies,[8−10,16−27] but in practice this is usually achieved via post-polymerization processing in dilute aqueous solution, often with the aid of a water-miscible co-solvent or a pH switch. Notwithstanding the important advances described above, the efficient synthesis of bespoke block copolymer nanoparticles with well-defined morphologies in concentrated aqueous solution is widely recognized to be a formidable technical challenge. Recently, Charleux and co-workers have made considerable progress toward this important scientific objective utilizing various *emulsion polymerization* formulations.[28,29] Thus, a water-soluble polymer precursor is chain-extended by polymerizing a *water-immiscible* monomer such as styrene, methyl methacrylate, or *n*-butyl acrylate via living radical polymerization[29−31] so as to produce an amphiphilic diblock copolymer in situ. This approach leads to polymerization-induced self-assembly (PISA) and can produce diblock copolymer nanoparticles in the form of either spheres, worms (sometimes described as "fibers"), or vesicles, with the final copolymer morphology being dictated primarily by the relative volume fractions of the hydrophilic and hydrophobic blocks.[9,18]

AQUEOUS DISPERSION POLYMERIZATION

In contrast to aqueous emulsion polymerization, this Perspective is focused on a versatile alternative approach to aqueous emulsion polymerization known as *aqueous dispersion polymerization*. An important prerequisite for such formulations is the selection of a *water-miscible* monomer which, when polymerized, forms a *water-insoluble* polymer. Normally, this would simply lead to macroscopic precipitation, but stable colloidal dispersions can be obtained if an appropriate colloid stability mechanism prevails.[32] In practice, this is readily achieved via chain extension of a suitable water-soluble polymer, which acts as a steric stabilizer to prevent precipitation of the growing water-insoluble block (see Scheme 1).[33] These aqueous dispersion polymerizations are conducted using reversible addition−fragmentation chain transfer (RAFT) chemistry, which is a type of living radical polymerization. RAFT polymerization is based on *rapid reversible chain transfer* between polymer radicals and organosulfur-based chain-transfer agents (CTAs), such as dithiobenzoates, trithiocarbonates, or

Scheme 1. Principle of Polymerization-Induced Self-Assembly Conducted in Aqueous Media[a]

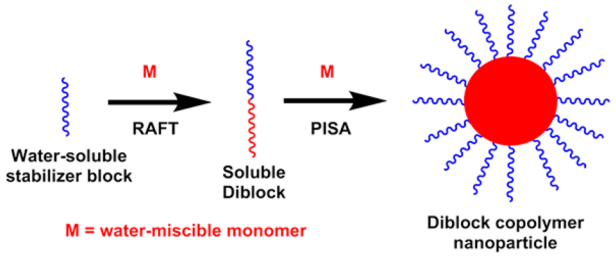

[a]A water-soluble stabilizer block is chain-extended using a water-miscible monomer via RAFT polymerization. Initially, a soluble diblock copolymer is obtained, but at some critical degree of polymerization the growing second block becomes water-insoluble, which causes in situ self-assembly. In this case only a spherical morphology is depicted, but other morphologies are also possible (see later).

Received: March 20, 2014
Published: June 26, 2014

   dx.doi.org/10.1021/ja502843f | J. Am. Chem. Soc. 2014, 136, 10174−10185

xanthates.[34−36] This enables the controlled polymerization of *functional* vinyl monomers while minimizing the termination reactions that would otherwise result in loss of control.

It is perhaps noteworthy that both McCormick's group[57] and Laschewsky and co-workers[58] have reported that RAFT polymer chain-ends can be susceptible to hydrolysis when RAFT polymerizations are conducted in water, particularly above pH 7. In this regard, there is some evidence that dithiobenzoates are more susceptible to *in situ* hydrolysis than trithiocarbonates.[59] However, in the context of RAFT aqueous dispersion polymerization, we find that both dithiobenzoates and trithiocarbonates give high monomer conversions, good blocking efficiencies, and low final copolymer polydispersities (typically M_w/M_n < 1.20), provided that these syntheses are conducted in mildly acidic aqueous solution (pH 3−6).

In practice, relatively few vinyl monomers are amenable to aqueous dispersion polymerization: literature examples include *N*-isopropylacrylamide (NIPAM),[37,38] *N,N′*-diethylacrylamide (DEAA),[39] 2-methoxyethyl acrylate (MEA),[40,41] 2-hydroxypropyl methacrylate (HPMA),[42,43] and di(ethylene glycol) methyl ether methacrylate (DEGMA).[44,45] The chemical structures of these five monomers are shown in Scheme 2. In each case the corresponding homopolymer has relatively weak hydrophobic character, which means that the resulting diblock copolymer nanoparticles exhibit varying degrees of thermo-sensitivity. This stimulus-responsive behavior is *not* exhibited by more hydrophobic polymers such as polystyrene or poly(methyl methacrylate).[29,31] As we shall see later, this property leads directly to additional opportunities for technological applications, particularly in the biomedical field.

Scheme 2. Chemical Structures of Five Water-Miscible Vinyl Monomers for Which Each Corresponding Homopolymer Is Water-Insoluble[a]

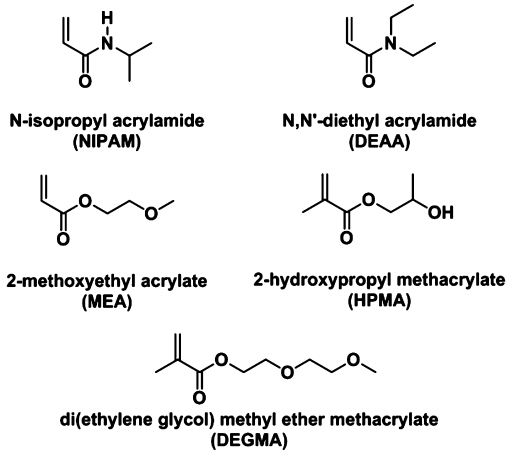

[a]Such monomers form a relatively small subset of building blocks that fulfill the essential requirements for an aqueous dispersion polymerization formulation.

With the exception of HPMA, only *spherical* nanoparticles have been obtained when using the monomers depicted in Scheme 2 to generate the core-forming block in RAFT aqueous dispersion polymerization formulations.[38−40,46]

The first report of RAFT aqueous dispersion polymerization was published by Hawker and co-workers,[38] who prepared poly(*N,N′*-dimethylacrylamide)−poly(*N*-isopropylacrylamide) diblock copolymer nanoparticles via RAFT aqueous dispersion polymerization with the aid of microwave irradiation, with the further addition of a bis(acrylamide) cross-linker during the NIPAM polymerization producing thermo-responsive nanogels. In the same year, Charleux and co-workers[39b] described the synthesis of similar nanogels with the core-forming block based on DEAA rather than NIPAM using nitroxide-mediated polymerization.

More recently, An and co-workers have reported the synthesis of further examples of thermo-sensitive nanogels using RAFT aqueous dispersion polymerization.[40,41,44] For example, a poly(oligo(ethylene glycol) methyl ether methacrylate) macromolecular chain-transfer agent (macro-CTA) was chain-extended with MEA[41] in the presence of a poly(ethylene glycol) diacrylate cross-linker at 30−40 °C using a low-temperature initiator (see Figure 1a). Spherical

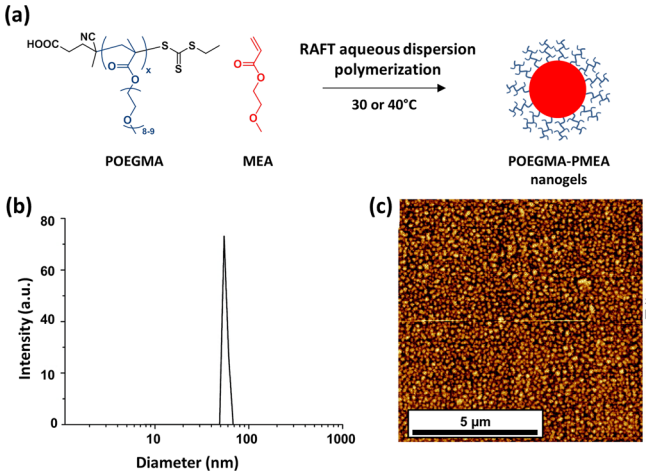

Figure 1. (a) Synthesis of spherical diblock copolymer nanogels via RAFT aqueous dispersion polymerization at 30 or 40 °C. (b) Intensity average size distribution obtained using DLS. (c) AFM image of the dried nanogel particles. Adapted with permission from ref 41.

block copolymer nanogels were obtained at up to 32% solids with very high monomer conversions being achieved. Dynamic light scattering (DLS) studies indicated relatively narrow size distributions (see Figure 1b) and mean hydrodynamic diameters ranging from 40 to 60 nm. Atomic force microscopy (AFM) studies were also undertaken, which were consistent with the DLS data (see Figure 1c). In a second study, the stabilizer block comprised either linear poly(ethylene glycol) or poly(oligo(ethylene glycol) methyl ether methacrylate), while the core-forming block was a statistical copolymer of oligo(ethylene glycol) methyl ether methacrylate, di(ethylene glycol) methyl ether methacrylate), and a small amount of poly(ethylene glycol) dimethacrylate.[44] The resulting nanogels had mean hydrodynamic diameters of 52−154 nm and relatively low polydispersities as judged by DLS studies, while variable-temperature ^{1}H NMR studies were used to characterize their thermo-responsive behavior.

Nanogels prepared using the branched copolymer stabilizer exhibited superior colloidal stability compared to the linear poly(ethylene glycol)-stabilized nanogels when subjected to a freeze−thaw cycle or when challenged using 100% fetal bovine serum. Moreover, high cell viabilities were obtained when A549 lung cells were exposed to these nanogels for 48 h, suggesting good biocompatibilities. In a third study,[40] similar nanogels were prepared via chain extension of a hydrophilic poly(*N,N′*-

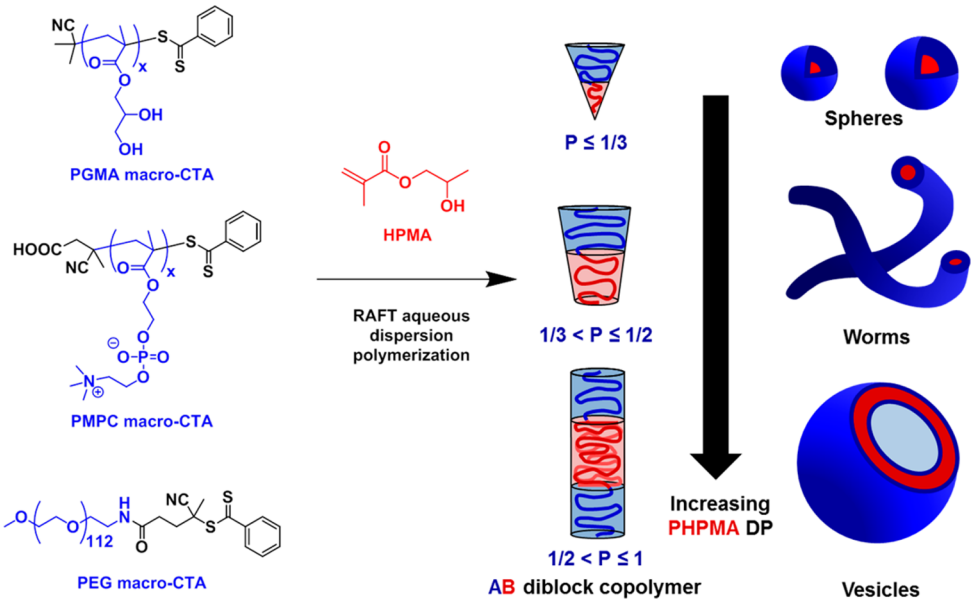

Figure 2. RAFT aqueous dispersion polymerization of 2-hydroxypropyl methacrylate using either a poly(glycerol monomethacrylate), poly[2-(methacryloyloxy)ethyl phosphorylcholine], or poly(ethylene glycol) macromolecular chain transfer agent to produce spheres, worms, or vesicles by judicious variation of the packing parameter, *P*, which is determined by the relative volume fractions of the stabilizer and core-forming blocks.[18]

dimethylacrylamide) macro-CTA using a mixture of mainly MEA along with poly(ethylene glycol) methyl ether acrylate and a small amount of poly(ethylene glycol) diacrylate cross-linker. According to DLS studies, the dimensions of such nanogels decrease almost linearly with increasing solution temperature, which is in marked contrast to the sharp thermal transitions exhibited by other thermo-responsive polymers, such as poly(*N*-isopropylacrylamide). In a related FT-IR spectroscopy study conducted by the same research group, these differing volume phase transitions have been interpreted in terms of subtle differences in hydrogen bonding between the core-forming blocks and the surrounding water molecules.[47]

A PROTOTYPICAL RAFT AQUEOUS DISPERSION POLYMERIZATION FORMULATION FOR DIBLOCK COPOLYMER NANO-OBJECTS

Notwithstanding these seminal contributions by others, currently the most versatile RAFT aqueous dispersion polymerization formulations are based on the chain extension of either a poly(glycerol monomethacrylate) [PGMA], poly(2-(methacryloyloxy)ethyl phosphorylcholine) [PMPC], or poly(ethylene glycol) [PEG] macro-CTA with HPMA as the core-forming monomer (see Figure 2). This approach is currently the *only* protocol that provides access to non-spherical morphologies such as worms or vesicles (see TEM images in Figure 3). Moreover, it is typically characterized by high final monomer conversions (>99% within 2 h at 70 °C, see Figure 4a) and blocking efficiencies of at least 90%.[18,42] Relatively narrow molecular weight distributions (M_w/M_n < 1.20) can be routinely achieved, provided that the batch of HPMA monomer that is utilized does not contain too much dimethacrylate impurity.[42,48] If required, the HPMA monomer can be further purified prior to use via silica chromatography, although this is a relatively inefficient process. As the PHPMA chain grows from the water-soluble PGMA macro-CTA, at some point it reaches a critical degree of polymerization (DP) and becomes sufficiently hydrophobic so as to induce micellar nucleation. The precise onset of such nucleation depends on many

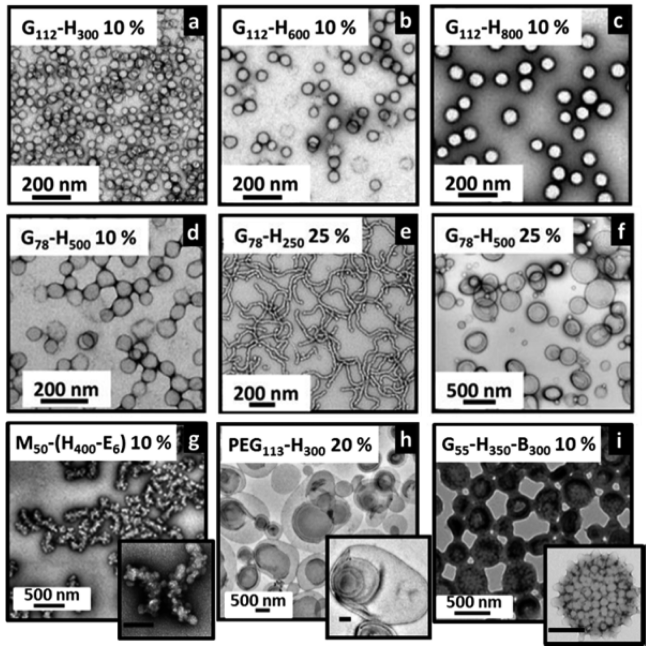

Figure 3. Representative transmission electron microscopy (TEM) images obtained for (a–c) a series of G_{112}-H_x spheres; (d–f) G_{78}-H_x spheres, worms, and vesicles synthesized at various concentrations; (g) M_{50}-(H_{400}-E_6) "lumpy rods"; (h) PEG_{113}-$PHPMA_{300}$ oligolamellar vesicles; and (i) G_{55}-H_{300}-B_{300} framboidal vesicles. Scale bar on inset images = 200 nm. For brevity, G, H, M, E, and B denote GMA, HPMA, MPC, EGDMA, and BzMA, respectively. Adapted with permission from refs 43, 52, and 70.

parameters, including the mean DP of the PGMA block, the initial HPMA concentration, the target DP of the PHPMA block, and the reaction temperature. For a RAFT aqueous dispersion polymerization conducted at 70 °C by Blanazs et al.,[42] micellar nucleation was observed by visual inspection at around 46% conversion when targeting a $PGMA_{47}$-$PHPMA_{200}$ diblock composition. This corresponds to a diblock composi-

dx.doi.org/10.1021/ja502843f | J. Am. Chem. Soc. 2014, 136, 10174–10185

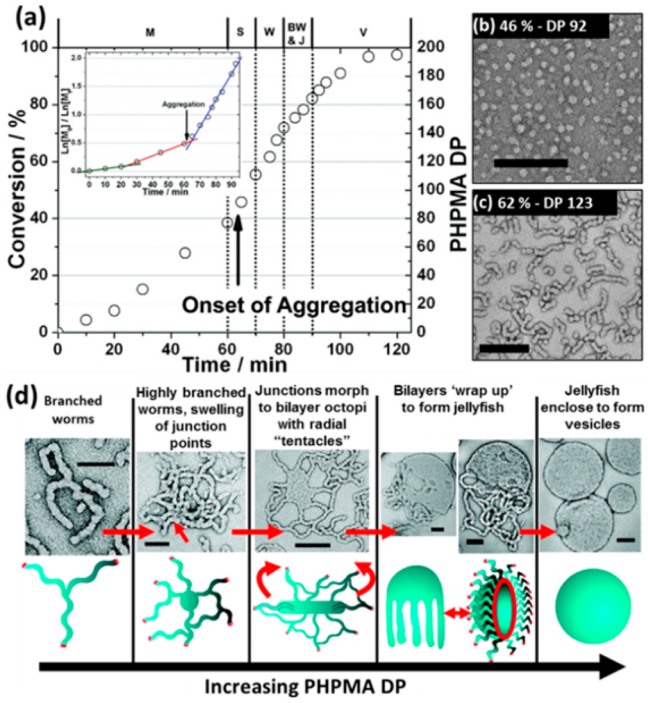

Figure 4. (a) HPMA polymerization kinetics obtained for the targeted G_{47}-H_{200} diblock copolymer nanoparticles (where G and H are shorthand for GMA and HPMA, respectively) prepared via RAFT aqueous dispersion polymerization at 70 °C and 10% w/w solids. According to TEM studies, the five morphological regimes are as follows: molecularly dispersed copolymer chains (M), spherical micelles (S), worms (W), branched worms (BW), jellyfish (J), and vesicles (V). The inset shows a semilogarithmic plot for a subset of these data, which confirms the five-fold *nucleation-induced* rate enhancement observed after micellar aggregation. (b) TEM image of spherical micelles at 46% HPMA conversion. (c) TEM image of worms at 62% HPMA conversion (scale bar = 100 nm). (d) Suggested mechanism for the worm-to-vesicle transformation during the synthesis of G_{47}-H_{200} by RAFT aqueous dispersion polymerization. Adapted with permission from ref 42.

tion of $PGMA_{47}$-$PHPMA_{92}$. This *in situ* self-assembly was confirmed by DLS analysis and TEM studies, which indicated the formation of approximately spherical nanoparticles of around 20−30 nm diameter (see Figure 4b). At this point, some of the 54% unreacted HPMA monomer becomes solubilized within the micelles, which leads to a relatively high local monomer concentration. This causes a five-fold rate acceleration as judged by ^{1}H NMR spectroscopy studies (see Figure 4a). As the monomer-swollen copolymer micelles grow, they undergo 1D fusion to form worms. In view of a recent theoretical study of the formation of long chains by spherical nanoparticles, such worm evolution appears to be an entropy-driven process.[49] The initially linear worms then become branched, and later "octopi" are formed (see Figure 4d). The flat patches that make up the latter copolymer morphology then begin to wrap up to produce "jellyfish", with the latter nanostructures comprising hemi-vesicles with worms dangling from the periphery. Further polymerization leads to vesicles inter-connected by long worms, with well-defined (albeit polydisperse) vesicles being the sole morphology that is observed at high HPMA conversions (>95%). This remarkable evolution in copolymer morphology, from relatively slow solution polymerization, to micellar nucleation to a final vesicular morphology occurs within 2 h at 70 °C. This change in copolymer morphology from spheres to worms to vesicles can be rationalized in terms of an increase in the packing parameter, P, which is given by the equation

$$P = v/al$$

For an amphiphilic AB diblock copolymer such as PGMA-PHPMA, v and l are the volume and the length of the hydrophobic block, respectively, and a is the effective interfacial area of the block junction. This concept was originally introduced by Israelachvili and co-workers[50] to explain surfactant self-assembly and was later extended to include diblock copolymer self-assembly by Antonietti and Förster.[16] It is generally accepted that spherical micelles are favored when $P \leq 0.33$, cylindrical micelles are produced when $0.33 < P \leq 0.50$, and vesicles are formed when $0.50 < P \leq 1.00$ (see Figure 2). In the context of this RAFT aqueous dispersion polymerization formulation, the mean DP of the PGMA stabilizer block is fixed, while the mean DP of the hydrophobic PHPMA block gradually increases as the HPMA polymerization proceeds. Thus P also necessarily increases during the synthesis, which accounts for the progressive evolution in copolymer morphology from spheres to worms to vesicles.[16,18]

However, this is merely a qualitative argument: calculation of P for diblock copolymers is non-trivial, particularly when both ^{1}H NMR studies[51] and small-angle X-ray scattering (SAXS) analysis[52] indicate that the core-forming (or membrane-forming) block is partially solvated with water molecules (in addition to unreacted monomer for intermediate conversions). Further theoretical studies in this area are clearly desirable, since they could enable predictions of the sphere/worm and worm/vesicles phase boundaries for yet-to-be-synthesized diblock copolymer nanoparticles.[53]

USING PHASE DIAGRAMS TO TARGET PURE COPOLYMER MORPHOLOGIES

A detailed post-mortem experimental phase diagram constructed for G_{78}-H_x (where G denotes PGMA and H denotes PHPMA) is shown in Figure 5.[18] On the basis of the extensive surfactant literature,[9,54,55] we anticipated that the amphiphile concentration should dictate the particle morphology, hence this is the parameter plotted on the x-axis. For a fixed PGMA stabilizer block DP of 78, systematic variation of the DP of the core-forming PHPMA block should generate a series of G_{78}-H_x diblock copolymers of differing packing parameters. To construct the phase diagram, TEM was used to assign the final copolymer morphology obtained at >99% HPMA monomer conversion. Only spherical nanoparticles are observed for RAFT polymerizations conducted at a copolymer concentration of 10% w/w, regardless of the target DP of the core-forming block. Moreover, the mean diameter of these spherical nanoparticles increases monotonically as the DP of the core-forming block is increased.

Similarly, only spherical nanoparticles are obtained at copolymer concentrations of up to 25% w/w, provided that the target DP of the core-forming block is below 150. To access higher order copolymer morphologies, longer core-forming blocks must be targeted at relatively high copolymer concentrations. This approach enables pure vesicular and worm phases to be generated. The former particles occupy a relatively broad phase region, whereas the latter occupy a relatively narrow phase region. Moreover, the worm phase is bounded by mixed phases (i.e., worms plus spheres or worms plus vesicles). Thus, reliable targeting of the worm phase

dx.doi.org/10.1021/ja502843f | J. Am. Chem. Soc. 2014, 136, 10174−10185

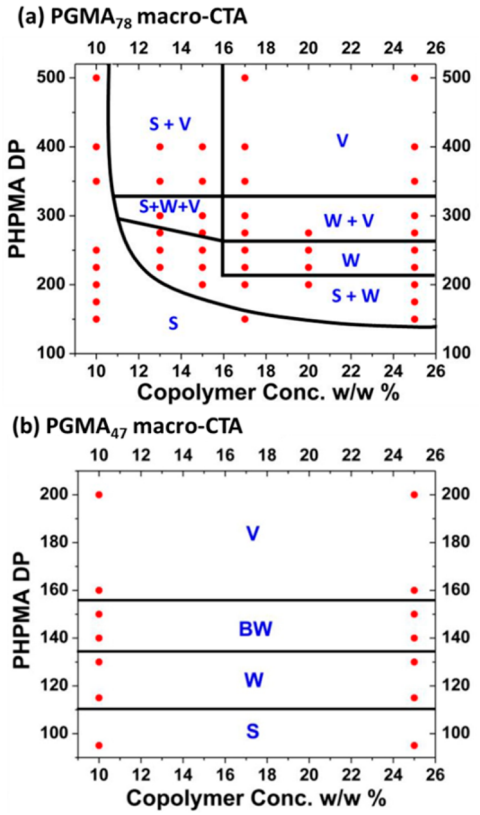

Figure 5. Phase diagrams obtained for a series of (a) G_{78}-H_x and (b) G_{47}-H_x copolymers synthesized by aqueous RAFT dispersion polymerization over copolymer concentrations ranging from 10% to 25% w/w. S = spherical micelles, W = worms, BW = branched worms, and V = vesicles. Adapted with permission from ref 43.

usually becomes feasible only after construction of a full phase diagram. At intermediate copolymer concentrations and core-forming block DPs, there is also a very narrow complex phase in which all three kinetically trapped copolymer morphologies coexist. Although such phase diagrams serve as a "roadmap" for the reproducible synthesis of pure copolymer morphologies, it should be emphasized that they are not equilibrium phase diagrams such as those reported for solid-state diblock copolymer morphologies.[56] Indeed, the spherical nanoparticles obtained on the left-hand side of the phase diagram (e.g., those prepared at 10% w/w solids) represent kinetically-trapped morphologies. This is best illustrated by considering the G_{78}-H_{500} copolymer prepared at 10% and 25% w/w solids. Gel permeation chromatography (GPC) analyses of these two samples confirm that essentially the same copolymer chains are obtained in each case ($M_n \approx$ 72K−74K, $M_w/M_n \approx 1.25$). However, the copolymer prepared at lower concentration forms spheres, whereas that formed at higher concentration forms vesicles. Clearly, only one of these two copolymers can be in its thermodynamically preferred equilibrium morphology. Based on the diblock asymmetry, the preferred morphology must be vesicles. If this is the case, then why does the G_{78}-H_{500} diblock copolymer remain trapped as spheres when prepared at 10% w/w solids? The initial event in the evolution of the copolymer morphology from spheres is the fusion of two spheres to form a spherical dimer. This is the critical first stage in the formation of worms, which eventually transform into vesicles via the sequence of events described above.[42] Presumably, the relatively long G_{78} stabilizer block confers sufficiently effective steric stabilization such that essentially no spherical micelle fusion events occur, at least on the time scale of the HPMA polymerization (2 h at 70 °C). In contrast, inelastic collisions that result in inter-micelle fusion are much more frequent at 25% w/w solids, which allows morphological evolution to occur on the time scale of the RAFT synthesis. On lowering the mean DP of the stabilizer block from 78 to 47, the steric barrier to micelle fusion is significantly reduced. This leads to a strikingly different phase diagram for a series of G_{47}-H_x diblock copolymers (see Figure 5b). In this case, there is essentially zero concentration dependence for the final copolymer morphology, which is now dictated solely by the target DP of the core-forming block. Vesicles can be readily obtained even at 10% w/w solids and at much lower core-forming block DPs than those required for the G_{78}-H_x formulation. On the other hand, *increasing* the DP of the stabilizer block to 112 leads to the formation of mainly spheres (see TEM images in Figure 3a−c), presumably because the steric barrier is now too high to allow efficient micelle fusion, even at copolymer concentrations as high as 25% w/w. Thus, although we currently have no quantitative understanding of the packing parameter *P* for these formulations, it is possible to qualitatively explain many experimental observations. However, it remains to be seen whether the phase diagram shown for G_{47} actually represents the *thermodynamically preferred* equilibrium states of the various copolymer chains.

MORE COST-EFFECTIVE FORMULATIONS

Glycerol monomethacrylate (GMA) is a commercially available specialty monomer that is used in the manufacture of soft contact lenses. It is prepared on an industrial scale from glycerol via protecting group chemistry using acetone to mask two of the three hydroxy groups.[60] As such, high-purity (i.e., low dimethacrylate content) GMA is relatively expensive compared to other hydroxy-functional comonomers such as HPMA. Thus it is worth considering alternative synthetic routes to GMA. For example, Ratcliffe and co-workers[48] recently described the convenient synthesis of GMA monomer in the form of an 11% w/w aqueous solution by simply heating a 10% w/w aqueous *emulsion* of glycidyl methacrylate (GlyMA) at 80 °C for 9 h at around pH 6. No background polymerization was detected by ^{1}H NMR spectroscopy when this reaction was conducted in the presence of dissolved oxygen, which acts as an inhibitor. Perhaps more surprisingly, no evidence for methacrylic ester hydrolysis was observed under these conditions. On cooling to 70 °C followed by deoxygenation via a nitrogen purge, the GMA was polymerized via RAFT aqueous solution polymerization to afford a near-monodisperse $PGMA_{45}$ macro-CTA, which could be subsequently chain-extended with HPMA to produce PGMA-PHPMA diblock copolymer spheres, worms, or vesicles. A one-pot formulation was also demonstrated for the overall process, although blocking efficiencies were somewhat lower than those observed for PGMA macro-CTAs isolated at intermediate conversions. Another restriction is the presence of somewhat higher levels of dimethacrylate cross-linker (>0.30 mol%) formed during the *in situ* conversion of GlyMA into GMA. This problem effectively limits the DP of the PGMA block that can be targeted; otherwise, its degree of branching/cross-linking compromises the subsequent PISA process.

dx.doi.org/10.1021/ja502843f | J. Am. Chem. Soc. 2014, 136, 10174−10185

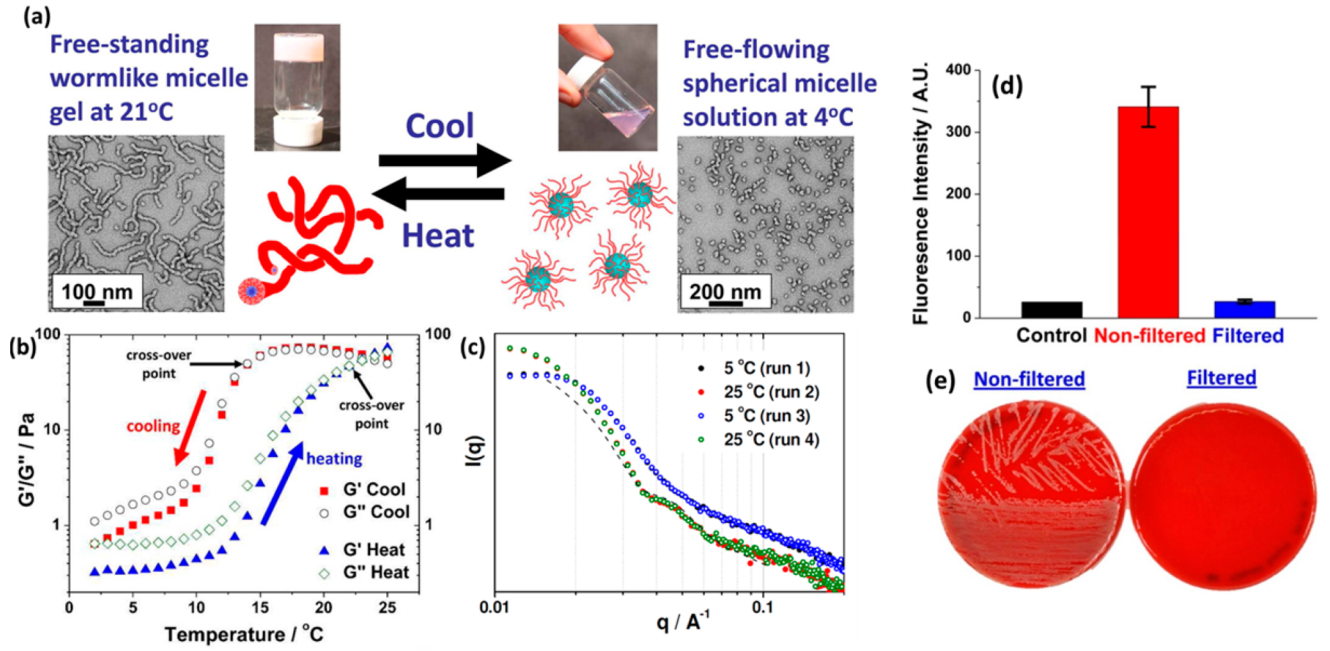

Figure 6. (a) Thermoresponsive aqueous solution behavior of a 10% w/w aqueous dispersion of G_{54}-H_{140} diblock copolymer particles. TEM studies of grids prepared from a dilute aqueous dispersion of G_{54}-H_{140} dried at either 21 or 4 °C showing the reversible worm-to-sphere transition. (b) Variation of storage (G', filled symbols) and loss (G'', open symbols) moduli for a G_{54}-H_{140} worm gel at 10 w/w % during temperature cycling at 1 °C min^{-1}: (i) cooling from 25 to 2 °C (G', filled red squares; G'', open black circles) and (ii) subsequent warming from 2 to 25 °C (G', filled blue triangles; G'', open green diamonds). (c) Small-angle X-ray scattering (SAXS) patterns recorded for a 10% w/w G_{54}-H_{140} aqueous dispersion, confirming the reversible nature of the worm-to-sphere transition after two consecutive temperature cycles between 5 and 25 °C. These SAXS plots overlay almost perfectly, indicating excellent reversibility for this thermal transition. The dashed curve shows a simulated SAXS pattern of long cylindrical rods (diameter = 22 nm, diameter polydispersity = 18%, mean length = 1000 nm) which is given for comparison with the experimental SAXS data obtained for worms. (d) Fluorescence observed before and after sterilization by ultrafiltration of an aqueous dispersion of G_{54}-H_{140} diblock copolymer after its deliberate contamination with FITC-labeled *S. aureus*. (e) Plate cultures of unfiltered and ultrafiltered copolymer gels obtained after incubation for 24 h at 37 °C. Clearly, substantial bacterial growth has occurred in the unfiltered copolymer gel. In contrast, no bacterial growth is observed for the ultrafiltered copolymer gel (right-hand image), indicating complete removal of *S. aureus*. Adapted with permission from ref 51.

THERMO-RESPONSIVE DIBLOCK COPOLYMER WORM GELS

The PGMA-PHPMA diblock copolymer worms form a soft, free-standing gel in aqueous solution at 20 °C. Rheological studies indicate typical G' values for such gels of around 10^2 Pa at a copolymer concentration of 10% w/w. The critical gelation temperature (CGT) can be conveniently tuned from 7 to 20 °C by simply varying the precise diblock composition, with longer PHPMA DPs favoring lower CGTs.[61] Preliminary studies suggest that the CGT has little or no concentration dependence, although further work is required here.[61] Originally the possibility of inter-worm entanglements was suggested,[62,64] which is an accepted gelation mechanism for small-molecule surfactant worms.[27,28] However, given the relatively short mean worm length, it is perhaps more likely that gelation is simply the result of multiple inter-worm contacts. To what extent hydrogen-bonding interactions may be important in this context has not yet been explored. These PGMA-PHPMA diblock copolymer worm gels exhibit unusual thermo-responsive behavior (see Figure 6). On cooling of the gel from 20 to 5 °C, degelation occurs to produce a free-flowing fluid of low viscosity. Combined TEM and SAXS studies confirm that this phase transition is the result of a worm-to-sphere transition. Variable-temperature ^{1}H NMR studies indicate that this *order*−*order* transition occurs because of the higher degree of hydration of the core-forming PHPMA block at 5 °C. Such thermo-sensitivity was previously reported by Madsen and co-workers for PHPMA-based triblock and diblock copolymers.[64−66] It is emphasized that in this context the PHPMA block differs significantly in its behavior from the PNIPAM, PDEAA, and PMEA core-forming blocks reported by others.[21,38,39,41,44] PHPMA *homopolymer* is invariably water-insoluble under all conditions: it is only when this weakly hydrophobic chain is conjugated to a second water-soluble block (e.g., PGMA) that its thermo-sensitivity is revealed.[51,52,61] This subtle difference leads to the observation of an *order*−*order* transition, rather than the *order*−*disorder* transitions that characterize PNIPAM, PDEAA and PMEA core-forming blocks (each of the latter dissolves molecularly in aqueous solution at 20 °C but becomes water-insoluble on heating because of their inverse temperature−solubility behavior). In this context, it is perhaps best to consider the greater (partial) degree of hydration of the PHPMA block observed on cooling as being the result of "surface plasticization" of the worms. This effect is just sufficient to shift the molecular packing parameter, P, from the relatively narrow range that favors worms ($0.33 < P \leq 0.50$) to that favoring spheres ($P \leq 0.33$). SAXS was used to study the worm-to-sphere transition exhibited by a 10% w/w aqueous dispersion of $PGMA_{54}$-$PHPMA_{140}$ diblock copolymer (see Figure 6c). Inspection of an $I(q)$ vs q plot at low q (Guinier regime) allows convenient discrimination between spherical (zero gradient) and worm (gradient close to −1, which is the value expected for rigid rods) morphologies. Moreover, SAXS patterns obtained for two thermal cycles between 5 and 25 °C

dx.doi.org/10.1021/ja502843f | J. Am. Chem. Soc. 2014, 136, 10174−10185

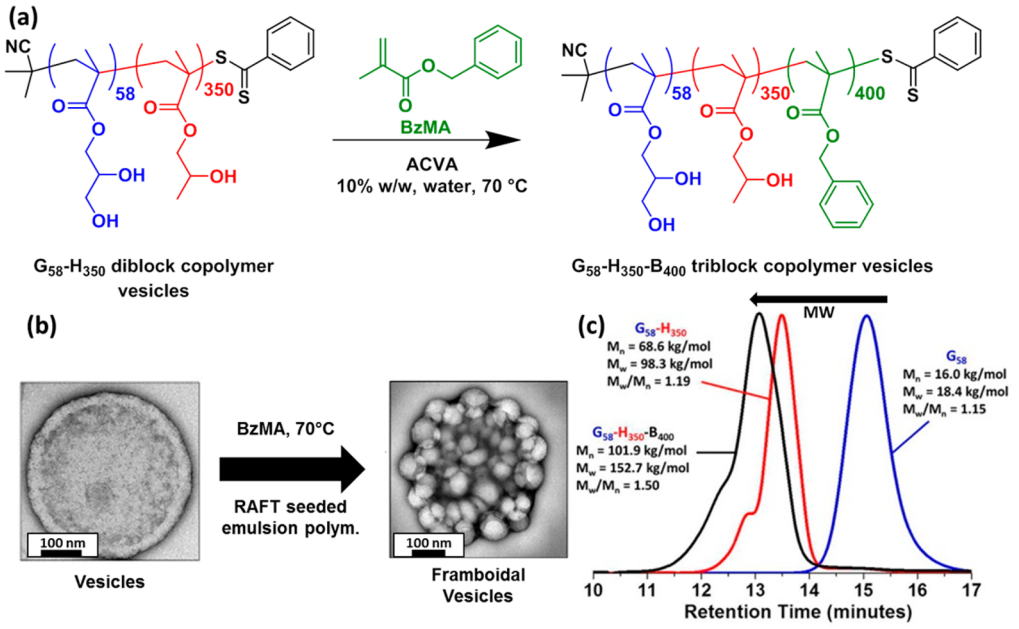

Figure 7. (a) Synthesis of a G_{58}-H_{350}-B_{400} triblock copolymer (where G, H, and B denote GMA, HPMA, and BzMA, respectively) via RAFT seeded emulsion polymerization of benzyl methacrylate from a G_{58}-H_{350} diblock precursor prepared by RAFT aqueous dispersion polymerization. (b) Evolution of morphology from conventional G_{58}-H_{350} vesicles to framboidal G_{58}-H_{350}-B_{400} vesicles. (c) Representative DMF GPC curves recorded for the G_{58} macro-CTA, G_{58}-H_{350} diblock and G_{58}-H_{350}-B_{400}triblock. Adapted with permission from ref 70.

proved to be almost perfectly superimposable, indicating that this morphological transition exhibits excellent reversibility in semi-concentrated aqueous solution. Further SAXS studies are now being conducted to examine whether this *order−order* transition remains fully reversible in more dilute aqueous solutions (1−5% w/w). The reversible worm-to-sphere transformation that occurs on cooling offers an opportunity for facile sterilization of the worm gels. This concept has been demonstrated by Blanazs and co-workers, who prepared a 10% w/w $PGMA_{54}$-$PHPMA_{140}$ worm gel loaded with a known quantity of a fluorescently labeled micro-organism (*Staphylococcus aureus*). On cooling to 5 °C, degelation was observed as expected, and the resulting cold aqueous dispersion was then passed through a 0.45 μm filter with the aid of a syringe. The relatively large bacteria (>0.50 μm diameter) were efficiently removed, while the much smaller diblock copolymer spheres (ca. 30−50 nm diameter) easily passed through the pores in the filter. On warming to 20 °C, the spheres reformed worms, which led to rapid re-gelation. Analysis of this gel using a fluorescence plate reader indicated that it contained essentially no bacteria, which was confirmed by subsequent bacterial culture experiments over 48 h (Figure 6d,e). It is emphasized that such cold-filter sterilization is aided by the relatively low viscosity of the spherical nanoparticles at 5 °C, which is not necessarily true for other diblock copolymer formulations.[67] This is directly related to the fact that the core-forming PHPMA block never becomes completely solvated at 5 °C, which prevents full molecular dissolution of the copolymer chains under these conditions. In principle, statistical copolymerization of more hydrophilic (or more hydrophobic) comonomers with HPMA should enable the CGT to be raised (or lowered), as desired. The critical gelation concentration appears to be around 3−4% w/w, as judged by tube inversion tests and gel rheology experiments. We are currently evaluating whether this observation is consistent with percolation theory.[68,69] If this turns out to be correct, it would support the hypothesis that gelation occurs simply because of inter-worm *contacts*. In contrast, inter-worm *entanglements* have been proposed as the gelation mechanism for surfactant worms.[62,63] Such contacts may well involve hydrogen bonding between PGMA stabilizer blocks on adjacent worms.

■ ABC TRIBLOCK COPOLYMER VESICLES

Chambon et al.[70] have examined the effect of adding a third comonomer to the prototypical RAFT aqueous dispersion polymerization formulation. In these experiments, $PGMA_{58}$-$PHPMA_{350}$ diblock copolymer vesicles were first prepared as a 10% w/w aqueous dispersion at 70 °C, and then a water-insoluble monomer such as ethylene glycol dimethacrylate (EGDMA) or benzyl methacrylate (BzMA) was added to the reaction solution after essentially full conversion of the HPMA. The resulting *in situ* polymerization is perhaps best described as a RAFT *seeded emulsion* polymerization, since the EGDMA or BzMA becomes solubilized within the hydrophobic PHPMA membrane of the vesicles. In the case of EGDMA, highly cross-linked vesicles were produced that can resist the addition of ionic surfactants such as sodium dodecyl sulfate, which cause immediate dissociation of the linear precursor vesicles.[71]

In the case of the BzMA comonomer, ABC triblock copolymer vesicles are obtained. In this case, the enthalpic incompatibility between the PHPMA and PBzMA blocks drives microphase separation within the vesicle membrane, leading to a series of remarkable *framboidal* vesicles (see Figures 3i and 7). Such morphologies are relatively rare in the literature;[72,73] the ability to prepare such well-defined nanoparticles at high solids via PISA formulations while exerting considerable control over the globule size (via systematic variation of the target DP of the PBzMA block) augurs well for potential applications that require nanoparticles of variable surface roughness.

Revisiting the cross-linked $PGMA_{58}$-$PHPMA_{350}$-$PEGDMA_{20}$ triblock copolymer vesicles described above, Thompson and co-workers[74] demonstrated that they were sufficiently robust to

dx.doi.org/10.1021/ja502843f | J. Am. Chem. Soc. 2014, 136, 10174−10185

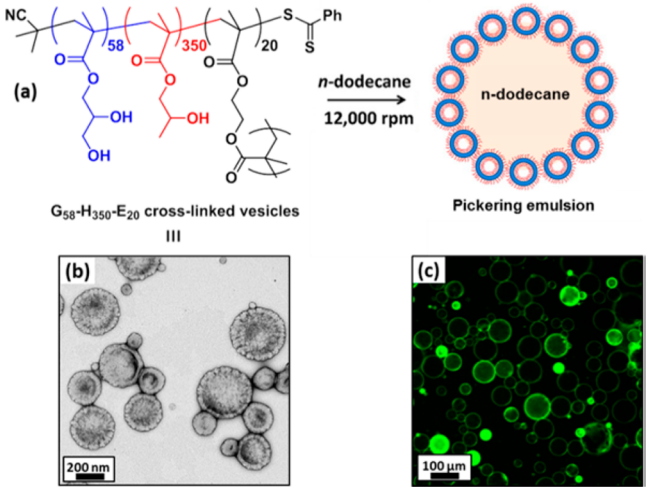

Figure 8. (a) Schematic representation of the preparation of Pickering emulsions using cross-linked G_{58}-H_{350}-E_{20} vesicles. (b) TEM image of cross-linked vesicles. (c) Fluorescence micrograph of colloidosomes obtained from a Pickering emulsion precursor prepared using fluorescein-labeled vesicles. Adapted with permission from ref 74.

act as Pickering emulsifiers, producing stable oil-in-water emulsions for a range of model oils (Figure 8). In contrast, control experiments confirmed that the *linear* $PGMA_{58}$-$PHPMA_{350}$ diblock copolymer precursor vesicles did not survive the high-shear conditions required for efficient homogenization of the oil and aqueous phases. Stable emulsions were again produced, but further investigation revealed that the oil droplets were merely stabilized by the individual diblock copolymer chains, rather than the original vesicles. Thus, using the EGDMA cross-linker appears to be *essential* for the production of genuine vesicle-based Pickering emulsions. Given that vesicles comprise mainly water, their Hamaker constants are relatively low compared to those of solid particles of the same dimensions, which suggests that only weak adsorption is likely at the oil/water interface. No doubt this accounts for their relatively inefficient adsorption, as judged by turbidimetric studies.[74] In principle, this problem might be overcome by preparing vesicles with greater surface roughness, since this parameter apparently leads to stronger interfacial adsorption.[75] However, it remains to be seen whether the framboidal vesicles described above offer any significant advantages in this regard.[76] Chambon and co-workers[71] explored an alternative post-polymerization cross-linking strategy whereby a minor fraction of glycidyl methacrylate (10%) was statistically copolymerized with HPMA when targeting a vesicular morphology. Approximately 90% of the epoxy groups survive under the RAFT polymerization conditions (2 h at 70 °C) and can be subsequently reacted with various water-soluble diamines to form highly cross-linked vesicles. The structural integrity of these vesicles was demonstrated by their resistance to added ionic surfactant, which causes rapid disintegration of the linear precursor vesicles. Rosselgong and co-workers[77] recently described the preparation of thiol-functional diblock copolymer vesicles via statistical copolymerization of a small amount of a disulfide-based dimethacrylate comonomer (DSDMA) with GMA during the synthesis of the macro-CTA. Provided that this copolymerization is conducted at relatively low concentration (10% solids), intramolecular cyclization is favored over intermolecular cross-linking.[78−80] This is important, because too high a degree of branching for the macro-CTA has a detrimental effect on the subsequent PISA synthesis. Once the precursor vesicles are prepared, the disulfide bonds within the stabilizer chains can be selectively cleaved under mild conditions to generate the desired thiol groups. Hence, although this route involves protecting group chemistry, it is actually highly atom-efficient. In principle, such thiol-functionalized vesicles may offer biomedical applications for mucoadhesion.[81] Thiol groups can also serve as orthogonal functionalities for decorating the vesicles with fluorescent groups or introducing cationic character.[77]

■ OTHER WATER-SOLUBLE MACRO-CTAS

Alternative steric stabilizer blocks to PGMA macro-CTAs include zwitterionic PMPC and non-ionic PEG. The former block comprises a relatively massive monomer repeat unit (295 g mol^{-1}). This means that the mean target DP of the PMPC macro-CTA has to be quite low (~25) in order to observe the full range of copolymer morphologies (i.e., spheres, worms, and vesicles). In contrast, higher DPs only allow access to spheres. Introducing an EGDMA cross-linker during the HPMA polymerization can lead to the formation of a rather unusual "lumpy rod" morphology (see Figure 3g).

PEG macro-CTAs can be prepared by end-group modification of the corresponding commercial monomethoxy-capped PEG precursor.[28,29,31,82,83] This is an attractive steric stabilizer block since it is highly biocompatible, and indeed there are already a number of FDA-approved PEGylated therapeutic entities.[84,85] In principle, preparing a macro-CTA from a well-defined precursor via end-group modification (rather than by RAFT polymerization) offers an important advantage, since there should be minimal batch-to-batch variation in its mean DP. In contrast, quenching a RAFT polymerization at intermediate conversion, which is desirable to prevent loss of RAFT end-groups under monomer-starved conditions, makes the *reproducible* targeting of a specific DP for a (meth)acrylic RAFT macro-CTA rather problematic.

It was found empirically that, when using a PEG_{113} macro-CTA for the aqueous dispersion polymerization of HPMA, the reaction temperature had to be reduced from 70 to 50 °C. The latter reaction temperature was preferred because it gave the lowest copolymer polydispersity, presumably because of the poor solubility of the PEG_{113} macro-CTA in hot aqueous solution. PEG_{113}-$PHPMA_x$ spheres, worms, or vesicles could be obtained, depending on the target DP (x) for the core-forming PHPMA block and the copolymer concentration. A detailed phase diagram was constructed for this new diblock copolymer formulation, with oligolamellar vesicles (see Figure 3h) being obtained at higher copolymer concentrations (>17.5% w/w). SAXS studies enabled characterization of this latter phase, indicating the presence of three concentric vesicles on average.[52] PEG_{113}-$PHPMA_x$ nano-objects also exhibited thermo-responsive behavior, but this proved to be qualitatively different from that observed for PGMA-PHPMA nano-objects. For example, a vesicle-to-sphere transition was observed on rapid cooling from 20 to 5 °C. Subsequent warming to 50 °C led to the formation of vesicles that were significantly smaller and less polydisperse than the original vesicles, as judged by DLS and TEM studies.

Moreover, this thermally induced vesicle−sphere−vesicle morphology cycle could be exploited to encapsulate a fluorescently labeled water-soluble polymer within the smaller vesicles. Rank et al.[86] reported similar thermo-sensitive

dx.doi.org/10.1021/ja502843f | J. Am. Chem. Soc. 2014, 136, 10174−10185

behavior for PEG-poly(2-vinylpyridine) vesicles prepared in dilute aqueous solution via post-polymerization processing. This suggests that RAFT-mediated PISA syntheses and traditional block copolymer processing strategies offer similar opportunities for the formation of stimulus-responsive vesicles.

POLYELECTROLYTE-STABILIZED NANO-OBJECTS

Highly anionic or cationic diblock copolymer nano-objects can be prepared via RAFT-mediated PISA using an appropriate polyelectrolytic macro-CTA based on either poly(potassium 3-sulfopropyl methacrylate) (PKSPMA) or quaternized poly(2-(dimethylamino)ethyl methacrylate), respectively.[59,87] For such syntheses, the addition of salt is usually beneficial since it screens the lateral electrostatic repulsive forces between the highly charged stabilizer chains, which otherwise impedes efficient PISA.

Nevertheless, such formulations appear to be restricted to spherical morphologies.[59,87] If worms or vesicles are desired, the most versatile approach appears to be the use of a binary mixture of a non-ionic PGMA macro-CTA with the desired polyelectrolytic macro-CTA (see Figure 9). This seems to be

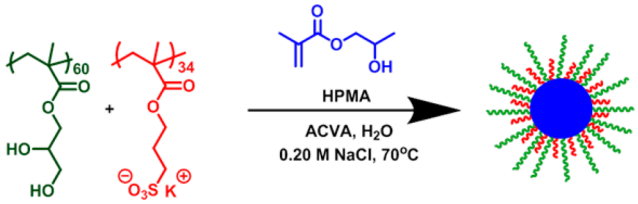

Figure 9. RAFT aqueous dispersion polymerization of HPMA using a binary mixture of $PKSPMA_{34}$ and $PGMA_{60}$ macro-CTAs to produce anionic diblock copolymer nano-objects. Adapted with permission from ref 87.

rather more useful than the statistical copolymerization of the desired ionic monomer with either GMA or 2-hydroxyethyl methacrylate (HEMA). Electrophoretic mobility measurements confirm the highly charged nature of the resulting nano-objects, while also providing good evidence for entropic mixing of the ionic and non-ionic macro-CTAs within the same nanoparticles.[59,87] Recently, Ladmiral and co-workers[88] also exploited this binary mixture of macro-CTAs approach in order to prepare a range of galactose-functional diblock copolymer nano-objects. In this case a poly(galactose methacrylate) (PGalSMA) macro-CTA was used in conjunction with a PGMA macro-CTA, with PHPMA being the core-forming block. More specifically, utilizing a 9:1 $PGMA_{51}$/$PGalSMA_{34}$ molar ratio allowed the synthesis of well-defined spheres, worms, or vesicles, depending on the target DP of the core-forming block. A turbidimetric assay confirmed that these galactose-functionalized nano-objects interacted strongly with RCA_{120}, which is a galactose-specific lectin (galectin). In contrast, control experiments confirmed no galectin interaction occurred for the corresponding PGMA-PHPMA nano-objects. Moreover, the sensitivity of this assay was strongly dependent on the copolymer morphology, with vesicles proving to be much more sensitive than worms or spheres. Finally, the interaction of the PGalSMA-containing vesicles with the cells could be used to efficiently deliver rhodamine B octadecyl ester into human dermal fibroblasts, presumably via interaction with galectins which are present in the extracellular space.[88]

FUTURE RESEARCH DIRECTIONS

One important extension of the current state-of-the-art would be the synthesis and evaluation of further examples of *stimulus-responsive* diblock copolymer nano-objects. In particular, pH-responsive nanoparticles should be accessible, perhaps based on certain amine-functional monomers such as 2-(*N*-morpholino)-ethyl methacrylate (MEMA) or 2-(diisopropylamino)ethyl methacrylate (DPA). In this context, it is probably important for the conjugate acid form of such basic monomers to possess a pK_a value below 7, since RAFT polymerizations usually suffer from side reactions when conducted in alkaline media.[57,58] For example, MEMA is water-miscible in its non-protonated form, which fulfills the fundamental criterion for an aqueous dispersion polymerization. In contrast, DPA is water-immiscible; hence, its use in this context would most likely require RAFT seeded emulsion polymerization.[70] Alternatives to the five monomers shown in Scheme 1 for the core-forming block would also be desirable, since this should lead to new thermo-responsive behavior.[89] In principle, other stimuli such as ionic strength or radiation (e.g., visible light) could also be technically feasible.[90]

It would be particularly useful to develop the theoretical framework for PISA. However, this will most likely be a non-trivial problem, because some copolymer morphologies are clearly kinetically trapped, whereas others appear to be thermodynamically controlled. It is already clear that the copolymer concentration, and possibly the rate of polymerization, is important in dictating the final copolymer morphology, and *in situ* monomer plasticization seems to play a critical role in determining the mobility of the core-forming block. Nevertheless, theoretical calculation of the relative volume fractions of the hydrophilic and hydrophobic blocks for given target degrees of polymerization should be attempted. Unfortunately, even this seemingly straightforward task is complicated by the non-negligible degree of hydration of the core-forming block. This latter parameter has been recently estimated to be of the order of 50% for PEG_{113}-$PHPMA_{300}$ diblock copolymer nano-objects on the basis of SAXS analysis.[52] Such scattering techniques are particularly powerful for characterization of block copolymer nano-objects.[52,91,92] In principle, a synchrotron X-ray source should enable SAXS to be used to monitor the entire PISA synthesis for the PGMA-PHPMA formulation. If the approach described by Blanazs et al.[42] is adopted, then such experiments should shed further light on the gradual evolution in particle morphology, from dissolved copolymer chains to monomer-swollen spherical micelles to worm formation via 1D micelle fusion to jellyfish intermediates through to the final vesicular morphology.

Given the recent advances in using SAXS to characterize framboidal colloidal nanocomposite particles,[93] it would also be interesting to use this technique to characterize the framboidal vesicles recently reported by Chambon et al.[70] Another technique that is expected to become important in future studies is cryo-TEM, which should be useful for further validation of the existence of some of the more transient copolymer morphologies, such as jellyfish and octopi.[42] In this context, it is worth emphasizing that the jellyfish observed in these RAFT aqueous dispersion polymerization syntheses are strikingly similar to the intermediate structures that can sometimes be observed during post-polymerization processing at high dilution (see Figure 10). This suggests that the jellyfish morphology observed during PISA represents a *generic*

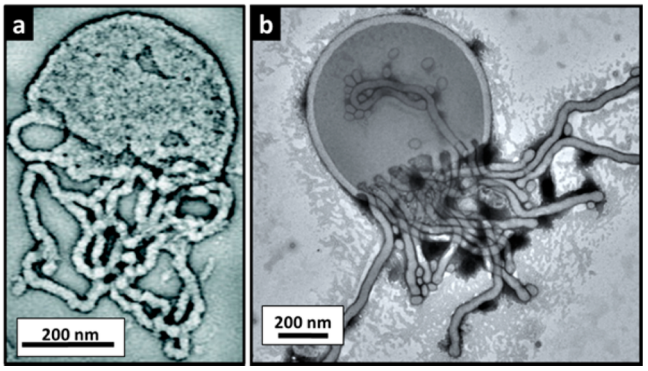

Figure 10. Transmission electron micrographs obtained for (a) a typical jellyfish intermediate observed during the synthesis of $PGMA_{47}$-$PHPMA_{200}$ vesicles via RAFT PISA at 70 °C (adapted with permission from ref 42) and (b) a similar species observed during the post-polymerization processing of a $PMPC_{25}$-$PDPA_{135}$ diblock copolymer via a solvent switch at 20 °C. The striking similarities between these structures suggest that such jellyfish are *generic* intermediates, rather than being merely an esoteric feature of the PISA process.

intermediate required for the evolution of worms into vesicles, rather than merely a specific feature of this self-assembly pathway. It is perhaps worth emphasizing that RAFT aqueous dispersion polymerization now enables diblock copolymer vesicles to be readily prepared in aqueous solution at 20−25% solids. Given that such vesicles are apparently formed via transient jellyfish-type intermediates, this suggests that *in situ* loading into such hemi-vesicles may be feasible. In this context, a useful model payload is expected to be 20 nm silica nanoparticles since these are readily detected by TEM, and, in principle, loading efficiencies could be quantified using thermogravimetric analysis (after removing any excess silica sol via centrifugation/redispersion of the much larger silica-loaded vesicles. However, the real long-term objective would be demonstration of the efficient encapsulation of globular proteins, antibodies, or enzymes, which would most likely require reducing the polymerization temperature from 70 to 37 °C to avoid undesirable *in situ* denaturation of the biological entity. Although a lower reaction temperature might perhaps retard the rate of polymerization because of the reduced radical flux, this problem can be alleviated, by using a suitable low-temperature initiator.[94] This approach was recently demonstrated for the aqueous dispersion polymerization of HPMA using a PEG_{113} macro-CTA. In this case the polymerization was conducted at 50 °C, but in principle this initiator can also be used at temperatures as low as 25 °C if the *in situ* encapsulation of biological molecules within vesicles is desired.[95] The biocompatible and readily sterilizable nature of the PGMA-PHPMA worm gels suggests their potential application as cost-effective sterilizable hydrogels for the long-term storage of mammalian cells. In principle, such synthetic gels can be tailored to mimic specific properties of the extra-cellular matrix by incorporation of bio-active additives.[96] Of particular interest here should be human stem cells, for which various alternative 2D and 3D hydrogels have been recently evaluated.[97−100] In this context, the thermally-induced worm-to-sphere transition that occurs on cooling to 5 °C is likely to be highly attractive as a cell-harvesting route for cell biologists, who routinely utilize (cold) centrifugation as a convenient cell isolation technique. The ability to fine-tune the mechanical strength and CGT of these worm gels may also be of interest for dictating the ultimate morphology of stem cells. For example, it has been reported that relatively soft gels tend to promote the proliferation of neurons, whereas stiffer gels result in bone cell formation.[101] Similarly, raising the CGT up to 30 °C should minimize the thermal shock experienced by the cells during degelation.

It would be fascinating to examine the diblock copolymer worms as potential Pickering emulsifiers, and perhaps also as aqueous foam stabilizers. Velev and co-workers have previously used much larger fiber-like copolymer particles with considerable success,[102,103] but the typical dimensions of the diblock copolymer worms described herein are at least an order of magnitude smaller in both their mean worm lengths and worm widths. Given their highly convenient synthesis compared to other formulations,[20,104] diblock copolymer worms and vesicles generated via PISA are also likely to be attractive organic templates for the deposition of inorganic materials such as silica, magnetite or gold.

Finally, we note that the recent discovery[105] of the remarkably efficient occlusion of anionic block copolymer micelles within monolithic host crystals of $CaCO_3$ is likely to be fruitful for a range of PISA-synthesized anionic diblock copolymer nano-objects. In particular, we plan to examine whether anionic worms or vesicles can be incorporated into host crystals and, if so, to evaluate their effect on the mechanical properties of the resulting inorganic/organic nanocomposite materials.

■ CONCLUSIONS

In summary, the combination of PISA and RAFT aqueous dispersion polymerization clearly offers a remarkably broad technology platform for the rational design of bespoke block copolymer nano-objects. Indeed, given its efficiency, versatility, and potential scalability, this approach may well ultimately prove to be the *preferred synthetic route* for the preparation of many vinyl-based amphiphilic diblock copolymers for commercial applications.

■ AUTHOR INFORMATION

Corresponding Author

s.p.armes@sheffield.ac.uk

Notes

The authors declare no competing financial interest.

■ ACKNOWLEDGMENTS

S.P.A. acknowledges receipt of a five-year ERC Advanced Investigator grant (PISA 320372) and an EPSRC Platform grant (EP/J007846/1).

■ REFERENCES

(1) Szwarc, M. *Nature* **1956**, *178*, 1168.
(2) Szwarc, M.; Levy, M.; Milkovich, R. *J. Am. Chem. Soc.* **1956**, *78*, 2656.
(3) Newman, S. *J. Appl. Polym. Sci.* **1962**, *6*, S15.
(4) Krause, S. *J. Phys. Chem.* **1964**, *68*, 1948.
(5) Lewis, P. R.; Price, C. *Nature* **1969**, *223*, 494.
(6) Aggarwal, S. L. *Polymer* **1976**, *17*, 938.
(7) Hamley, I. W. *Angew. Chem., Int. Ed.* **2003**, *42*, 1692.
(8) Zhang, L.; Eisenberg, A. *Science* **1995**, *268*, 1728.
(9) Discher, D. E.; Eisenberg, A. *Science* **2002**, *297*, 967.
(10) Jain, S.; Bates, F. S. *Science* **2003**, *300*, 460.
(11) Kataoka, K.; Harada, A.; Nagasaki, Y. *Adv. Drug Delivery Rev.* **2001**, *47*, 113.

(12) Discher, B. M.; Won, Y.-Y.; Ege, D. S.; Lee, J. C.-M.; Bates, F. S.; Discher, D. E.; Hammer, D. A. *Science* **1999**, *284*, 1143.
(13) Ahmed, F.; Discher, D. E. *J. Controlled Release* **2004**, *96*, 37.
(14) Ahmed, F.; Pakunlu, R. I.; Srinivas, G.; Brannan, A.; Bates, F.; Klein, M. L.; Minko, T.; Discher, D. E. *Mol. Pharmaceutics* **2006**, *3*, 340.
(15) Lomas, H.; Canton, I.; MacNeil, S.; Du, J.; Armes, S. P.; Ryan, A. J.; Lewis, A. L.; Battaglia, G. *Adv. Mater.* **2007**, *19*, 4238.
(16) Antonietti, M.; Förster, S. *Adv. Mater.* **2003**, *15*, 1323.
(17) Bang, J.; Jain, S. M.; Li, Z. B.; Lodge, T. P.; Pedersen, J. S.; Kesselman, E.; Talmon, Y. *Macromolecules* **2006**, *39*, 1199.
(18) Blanazs, A.; Armes, S. P.; Ryan, A. J. *Macromol. Rapid Commun.* **2009**, *30*, 267.
(19) Cui, H.; Chen, Z.; Zhong, S.; Wooley, K. L.; Pochan, D. J. *Science* **2007**, *317*, 647.
(20) Wang, X.; Guerin, G.; Wang, H.; Wang, Y.; Manners, I.; Winnik, M. A. *Science* **2007**, *317*, 644.
(21) Charleux, B.; Delaittre, G.; Rieger, J.; D'Agosto, F. *Macromolecules* **2012**, *45*, 6753.
(22) Bütün, V.; Billingham, N. C.; Armes, S. P. *J. Am. Chem. Soc.* **1998**, *120*, 12135.
(23) Bütün, V.; Billingham, N. C.; Armes, S. P. *J. Am. Chem. Soc.* **1998**, *120*, 11818.
(24) Baines, F. L.; Armes, S. P.; Billingham, N. C.; Tuzar, Z. *Macromolecules* **1996**, *29*, 8151.
(25) Gilroy, J. B.; Lunn, D. J.; Patra, S. K.; Whittell, G. R.; Winnik, M. A.; Manners, I. *Macromolecules* **2012**, *45*, 5806.
(26) Qiu, H.; Cambridge, G.; Winnik, M. A.; Manners, I. *J. Am. Chem. Soc.* **2013**, *135*, 12180.
(27) Jang, S. G.; Audus, D. J.; Klinger, D.; Krogstad, D. V.; Kim, B. J.; Cameron, A.; Kim, S.-W.; Delaney, K. T.; Hur, S.-M.; Killops, K. L.; Fredrickson, G. H.; Kramer, E. J.; Hawker, C. J. *J. Am. Chem. Soc.* **2013**, *135*, 6649.
(28) Rieger, J.; Stoffelbach, F. o.; Bui, C.; Alaimo, D.; Jérôme, C.; Charleux, B. *Macromolecules* **2008**, *41*, 4065.
(29) Rieger, J.; Osterwinter, G.; Bui, C.; Stoffelbach, F.; Charleux, B. *Macromolecules* **2009**, *42*, 5518.
(30) Groison, E.; Brusseau, S.; D'Agosto, F.; Magnet, S.; Inoubli, R.; Couvreur, L.; Charleux, B. *ACS Macro Lett.* **2011**, *1*, 47.
(31) Boursier, T.; Chaduc, I.; Rieger, J.; D'Agosto, F.; Lansalot, M.; Charleux, B. *Polym. Chem.* **2011**, *2*, 355.
(32) Ali, A. M. I.; Pareek, P.; Sewell, L.; Schmid, A.; Fujii, S.; Armes, S. P.; Shirley, I. M. *Soft Matter* **2007**, *3*, 1003.
(33) Napper, D. H. *Polymeric Stabilization of Colloidal Dispersions*; Academic Press: London, 1983.
(34) Rizzardo, E.; Chiefari, J.; Chong, B. Y. K.; Ercole, F.; Krstina, J.; Jeffery, J.; Le, T. P. T.; Mayadunne, R. T. A.; Meijs, G. F.; Moad, C. L.; Moad, G.; Thang, S. H. *Macromol. Symp.* **1999**, *143*, 291.
(35) Moad, G.; Rizzardo, E.; Thang, S. H. *Aust. J. Chem.* **2009**, *62*, 1402.
(36) Moad, G.; Rizzardo, E.; Thang, S. H. *Aust. J. Chem.* **2005**, *58*, 379.
(37) An, Z.; Tang, W.; Hawker, C. J.; Stucky, G. D. *J. Am. Chem. Soc.* **2006**, *128*, 15054.
(38) An, Z. S.; Shi, Q. H.; Tang, W.; Tsung, C. K.; Hawker, C. J.; Stucky, G. D. *J. Am. Chem. Soc.* **2007**, *129*, 14493.
(39) (a) Grazon, C.; Rieger, J.; Sanson, N.; Charleux, B. *Soft Matter* **2011**, *7*, 3482. (b) Delaittre, G.; Save, M.; Charleux, B. *Macromol. Rapid Commun.* **2007**, *28*, 1528.
(40) Liu, G.; Qiu, Q.; An, Z. *Polym. Chem.* **2012**, *3*, 504.
(41) Liu, G.; Qiu, Q.; Shen, W.; An, Z. *Macromolecules* **2011**, *44*, 5237.
(42) Blanazs, A.; Madsen, J.; Battaglia, G.; Ryan, A. J.; Armes, S. P. *J. Am. Chem. Soc.* **2011**, *133*, 16581.
(43) Blanazs, A.; Ryan, A. J.; Armes, S. P. *Macromolecules* **2012**, *45*, 5099.
(44) Shen, W.; Chang, Y.; Liu, G.; Wang, H.; Cao, A.; An, Z. *Macromolecules* **2011**, *44*, 2524.
(45) Very recently, Monteiro and co-workers reported the preparation of diblock copolymer worms (and rods) decorated with a wide range of functional groups via the PNIPAM stabilizer chains using alkyne−azide chemistry: Jia, Z.; Bobrin, V. A.; Truong, N. P.; Gillard, M.; Monteiro, M. J. *J. Am. Chem. Soc.* **2014**, *136*, 5824. However, close reading of the experimental protocol used in this work indicates that this formulation is actually best described as a *surfactant-stabilized RAFT emulsion polymerization* (with styrene as the water-immiscible monomer and sodium dodecyl sulfate utilized as the anionic surfactant) rather than the RAFT aqueous dispersion polymerization claimed by the authors.
(46) Rieger, J.; Grazon, C.; Charleux, B.; Alaimo, D.; Jérôme, C. *J. Polym. Sci., Part A: Polym. Chem.* **2009**, *47*, 2373.
(47) Hou, L.; Ma, K.; An, Z.; Wu, P. *Macromolecules* **2014**, *47*, 1144.
(48) Ratcliffe, L. P. D.; Ryan, A. J.; Armes, S. P. *Macromolecules* **2013**, *46*, 769.
(49) Termonia, Y. *Colloids Surf., A* **2014**, *447*, 23.
(50) Israelachvili, J. N.; Mitchell, D. J.; Ninham, B. W. *J. Chem. Soc., Faraday Trans. 2: Mol. Chem. Phys.* **1976**, *72*, 1525.
(51) Blanazs, A.; Verber, R.; Mykhaylyk, O. O.; Ryan, A. J.; Heath, J. Z.; Douglas, C. W. I.; Armes, S. P. *J. Am. Chem. Soc.* **2012**, *134*, 9741.
(52) Warren, N. J.; Mykhaylyk, O. O.; Mahmood, D.; Ryan, A. J.; Armes, S. P. *J. Am. Chem. Soc.* **2014**, *136*, 1023.
(53) LaRue, I.; Adam, M.; Pitsikalis, M.; Hadjichristidis, N.; Rubinstein, M.; Sheiko, S. S. *Macromolecules* **2005**, *39*, 309.
(54) Shen, H.; Eisenberg, A. *J. Phys. Chem. B* **1999**, *103*, 9473.
(55) Broome, F. K.; Hoerr, C. W.; Harwood, H. J. *J. Am. Chem. Soc.* **1951**, *73*, 3350.
(56) Khandpur, A. K.; Foerster, S.; Bates, F. S.; Hamley, I. W.; Ryan, A. J.; Bras, W.; Almdal, K.; Mortensen, K. *Macromolecules* **1995**, *28*, 8796.
(57) McCormick, C. L.; Lowe, A. B. *Acc. Chem. Res.* **2004**, *37*, 312.
(58) Herfurth, C.; Malo de Molina, P.; Wieland, C.; Rogers, S.; Gradzielski, M.; Laschewsky, A. *Polym. Chem.* **2012**, *3*, 1606.
(59) Semsarilar, M.; Ladmiral, V.; Blanazs, A.; Armes, S. P. *Langmuir* **2012**, *28*, 914.
(60) Save, M.; Weaver, J. V. M; Armes, S. P.; McKenna, P. *Macromolecules* **2002**, *35*, 1152.
(61) Verber, R.; Blanazs, A.; Armes, S. P. *Soft Matter* **2012**, *8*, 9915.
(62) Cates, M. E. *J. Phys.: Condens. Matter* **1996**, *8*, 9167.
(63) Clausen, T. M.; Vinson, P. K.; Minter, J. R.; Davis, H. T.; Talmon, Y.; Miller, W. G. *J. Phys. Chem.* **1992**, *96*, 474.
(64) Madsen, J.; Armes, S. P.; Bertal, K.; Lomas, H.; MacNeil, S.; Lewis, A. L. *Biomacromolecules* **2008**, *9*, 2265.
(65) Madsen, J.; Armes, S. P.; Bertal, K.; MacNeil, S.; Lewis, A. L. *Biomacromolecules* **2009**, *10*, 1875.
(66) Madsen, J.; Armes, S. P.; Lewis, A. L. *Macromolecules* **2006**, *39*, 7455.
(67) Duval, M.; Waton, G.; Schosseler, F. *Langmuir* **2005**, *21*, 4904.
(68) Chatterjee, A. P. *J. Chem. Phys.* **2010**, *132*, 224905/1.
(69) Otten, R. H. J.; van, d. S. P. *J. Chem. Phys.* **2011**, *134*, 094902/1.
(70) Chambon, P.; Blanazs, A.; Battaglia, G.; Armes, S. P. *Macromolecules* **2012**, *45*, 5081.
(71) Chambon, P.; Blanazs, A.; Battaglia, G.; Armes, S. P. *Langmuir* **2013**, *28*, 1196.
(72) Zhao, W.; Chen, D.; Hu, Y.; Grason, G. M.; Russell, T. P. *ACS Nano* **2010**, *5*, 486.
(73) Brannan, A. K.; Bates, F. S. *Macromolecules* **2004**, *37*, 8816.
(74) Thompson, K. L.; Chambon, P.; Verber, R.; Armes, S. P. *J. Am. Chem. Soc.* **2012**, *134*, 12450.
(75) San-Miguel, A.; Behrens, S. H. *Langmuir* **2012**, *28*, 12038.
(76) Van Hest and co-workers have also recently explored the use of vesicles as novel Pickering stabilizers of water-in-oil emulsions, although in this case the vesicles were prepared via a traditional post-polymerization processing technique: Wang, Z.; van Oers, M. C. M.; Rutjes, F. P. J. T.; van Hest, J. C. M. *Angew. Chem., Int. Ed.* **2012**, *51*, 10746.

(77) Rosselgong, J.; Blanazs, A.; Chambon, P.; Williams, M.; Semsarilar, M.; Madsen, J.; Battaglia, G.; Armes, S. P. *ACS Macro Lett.* **2012**, *1*, 1041.
(78) Rosselgong, J.; Armes, S. P. *Macromolecules* **2012**, *45*, 2731.
(79) Rosselgong, J.; Armes, S. P.; Barton, W.; Price, D. *Macromolecules* **2009**, *42*, 5919.
(80) Rosselgong, J.; Armes, S. P.; Barton, W. R. S.; Price, D. *Macromolecules* **2010**, *43*, 2145.
(81) Bernkop-Schnürch, A. *Adv. Drug Delivery Rev.* **2005**, *57*, 1569.
(82) dos Santos, A. M.; Le Bris, T.; Graillat, C.; D'Agosto, F.; Lansalot, M. *Macromolecules* **2009**, *42*, 946.
(83) Bartels, J. W.; Cauet, S. I.; Billings, P. L.; Lin, L. Y.; Zhu, J. H.; Fidge, C.; Pochan, D. J.; Wooley, K. L. *Macromolecules* **2010**, *43*, 7128.
(84) Alconcel, S. N. S.; Baas, A. S.; Maynard, H. D. *Polym. Chem.* **2011**, *2*, 1442.
(85) Duncan, R. *Nat. Rev. Drug Discov.* **2003**, *2*, 347.
(86) Rank, A.; Hauschild, S.; Förster, S.; Schubert, R. *Langmuir* **2009**, *25*, 1337.
(87) Semsarilar, M.; Ladmiral, V.; Blanazs, A.; Armes, S. P. *Langmuir* **2013**, *29*, 7416.
(88) Ladmiral, V.; Semsarilar, M.; Canton, I.; Armes, S. P. *J. Am. Chem. Soc.* **2013**, *135*, 13574.
(89) Ratcliffe, L. P. D.; Blanazs, A.; Williams, C. N.; Brown, S. L.; Armes, S. P. *Polym. Chem.* **2014**, *5*, 3643.
(90) Stuart, M. A. C.; Huck, W. T. S.; Genzer, J.; Muller, M.; Ober, C.; Stamm, M.; Sukhorukov, G. B.; Szleifer, I.; Tsukruk, V. V.; Urban, M.; Winnik, F.; Zauscher, S.; Luzinov, I.; Minko, S. *Nat. Mater.* **2010**, *9*, 101.
(91) Pedersen, J. S.; Gerstenberg, M. C. *Colloids Surf. a: Physicochem. Eng. Aspects* **2003**, *213*, 175.
(92) Fielding, L. A.; Lane, J. A.; Derry, M. J.; Mykhaylyk, O. O.; Armes, S. P. *J. Am. Chem. Soc.* **2014**, *136*, 5790.
(93) Balmer, J. A.; Mykhaylyk, O. O.; Armes, S. P.; Fairclough, J. P. A.; Ryan, A. J.; Gummel, J.; Murray, M. W.; Murray, K. A.; Williams, N. S. J. *J. Am. Chem. Soc.* **2010**, *133*, 826.
(94) An, Z.; Qiu, Q.; Liu, G. *Chem. Commun.* **2011**, *47*, 12424.
(95) Boyer, C.; Bulmus, V.; Liu, J.; Davis, T. P.; Stenzel, M. H.; Barner-Kowollik, C. *J. Am. Chem. Soc.* **2007**, *129*, 7145.
(96) Griffith, L. G.; Swartz, M. A. *Nat. Rev. Mol. Cell Biol.* **2006**, *7*, 211.
(97) Lei, Y.; Schaffer, D. V. *Proc. Natl. Acad. Sci. U.S.A.* **2013**, *110*, E5039.
(98) Kouwer, P. H. J.; Koepf, M.; Le Sage, V. A. A.; Jaspers, M.; van Buul, A. M.; Eksteen-Akeroyd, Z. H.; Woltinge, T.; Schwartz, E.; Kitto, H. J.; Hoogenboom, R.; Picken, S. J.; Nolte, R. J. M.; Mendes, E.; Rowan, A. E. *Nature* **2013**, *493*, 651.
(99) Thiele, J.; Ma, Y.; Bruekers, S. M. C.; Ma, S.; Huck, W. T. S. *Adv. Mater.* **2014**, *26*, 125.
(100) Madl, C. M.; Mehta, M.; Duda, G. N.; Heilshorn, S. C.; Mooney, D. J. *Biomacromolecules* **2014**, *15*, 445.
(101) Engler, A. J.; Sen, S.; Sweeney, H. L.; Discher, D. E. *Cell* **2006**, *126*, 677.
(102) Alargova, R. G.; Paunov, V. N.; Velev, O. D. *Langmuir* **2005**, *22*, 765.
(103) Noble, P. F.; Cayre, O. J.; Alargova, R. G.; Velev, O. D.; Paunov, V. N. *J. Am. Chem. Soc.* **2004**, *126*, 8092.
(104) Groschel, A. H.; Walther, A.; Lobling, T. I.; Schacher, F. H.; Schmalz, H.; Muller, A. H. E. *Nature* **2013**, *503*, 247.
(105) Kim, Y.-Y.; Ganesan, K.; Yang, P.; Kulak, A. N.; Borukhin, S.; Pechook, S.; Ribeiro, L.; Kröger, R.; Eichhorn, S. J.; Armes, S. P.; Pokroy, B.; Meldrum, F. C. *Nat. Mater.* **2011**, *10*, 890.